ANL/ET/CP-99750

THERMAL IMAGING MEASUREMENT OF LATERAL THERMAL DIFFUSIVITY IN CONTINUOUS FIBER CERAMIC COMPOSITES[†]

J. G. Sun, C. Deemer, and W. A. Ellingson

Energy Technology Division
Argonne National Laboratory
Argonne, IL 60439

Paper to be presented at the American Ceramic Society's 24nd Annual Cocoa Beach Conference and Exposition: An International Conference on Engineering Ceramics and Structures, Cocoa Beach, FL, Jan. 23-28, 2000.

[†]Work sponsored by the U.S. Department of Energy, Energy Efficiency and Renewable Energy, Office of Industrial Technologies, under Contract W-31-109-ENG-38.

DISCLAIMER

DISCLAIMER

Portions of this document may be illegible in electronic image products. Images are produced from the best available original document.

THERMAL IMAGING MEASUREMENT OF LATERAL THERMAL DIFFUSIVITY IN CONTINUOUS FIBER CERAMIC COMPOSITES*

J. G. Sun, C. Deemer, and W. A. Ellingson

Argonne National Laboratory
Argonne, IL 60439

Infrared thermal imaging has become a common technique for nondestructive evaluation and measurement of thermal properties in ceramic specimens. Flash thermal imaging can be used to determine two-dimensional through-thickness thermal diffusivity in a planar specimen. In this study, we extended the method to determine lateral, or transverse, thermal diffusivity in the specimen. During the flash thermal imaging test, pulsed heat energy is applied to a specimen's back surface, which is partially shielded, and the change of temperature distribution on the front surface is monitored by an infrared thermal imaging system. The temperature distribution represents the effect of both the normal heat transfer through the specimen's thickness and the lateral heat transfer through the interface between the shielded and unshielded back-surface regions. Those temperature distributions are then fitted with a theoretical solution of the heat transfer process to determine the lateral thermal diffusivity at the interface. This technique has been applied to measure lateral thermal diffusivity in a steel plate and a continuous fiber ceramic composite specimen.

INTRODUCTION

Thermal diffusivity is a material property that relates to the transient heat transfer rate in a material. It is dependent on the heat transfer direction for anisotropic materials, such as continuous fiber ceramic composites (CFCCs). For planar samples, through-thickness (normal) thermal diffusivity can be determined easily by using a flash thermal imaging system that positions the sample between a flash lamp and an infrared camera (Parker, 1961; Sun et al., 1999). The present paper describes a new technique for determining lateral thermal diffusivity with an infrared thermal imaging system developed at Argonne National Laboratory.

One recently published method for measuring lateral thermal diffusivity (Ouyang et al., 1998) is based on a theory for semi-infinite-sized plates and requires fitting of the experimental data with the theoretical solution in the spatial domain. Because the quality of the curve fit is judged manually by the operator, uncertainty may result for the predicted lateral diffusivity. In addition, while low signal noise (e.g., due to variation of sensitivity for each infrared sensor at each pixel) can be filtered, the Ouyang et al. method cannot be used when high modulation of the data occurs as a possible result of optical-property variation on the sample surface. Our new technique solves all of these issues. It is based on an analytical solution for lateral heat transfer in finite-sized rectangular geometry, and the experimental data are fitted in both temporal and spatial domains by a computer code to determine the lateral thermal diffusivity and the interface position between the shielded and unshielded region.

EXPERIMENTAL SETUP

The thermal imaging system developed at Argonne is illustrated in Fig. 1. It consists of an infrared camera with a 256 x 256 focal-plane array of InSb detectors, a 200 MHz Pentium-based PC computer equipped with a high-speed digital frame grabber, and a function generator that produces an adjustable frame rate for the camera. The thermal impulse is applied with a photographic flash lamp system. A dual-timing trigger is used for simultaneous triggering of the flash lamps and data acquisition, while an analog video system is used to monitor the experiments.

During a flash thermal imaging test, pulsed heat energy is applied to the sample's back surface (at z = 0 as shown in Fig. 2), which is partially shielded, and the change of temperature distribution on the front surface (at z = L) is monitored by the infrared camera (see Figs. 2 and 3) that takes a series of thermal images to be stored in the PC. The temperature distribution represents the effect of both the normal heat transfer through the specimen's thickness and the lateral heat transfer through the interface between the shielded and unshielded regions. Those temperature distributions will then be fitted with an analytical solution of the heat transfer process to determine the lateral thermal diffusivity at the interface.

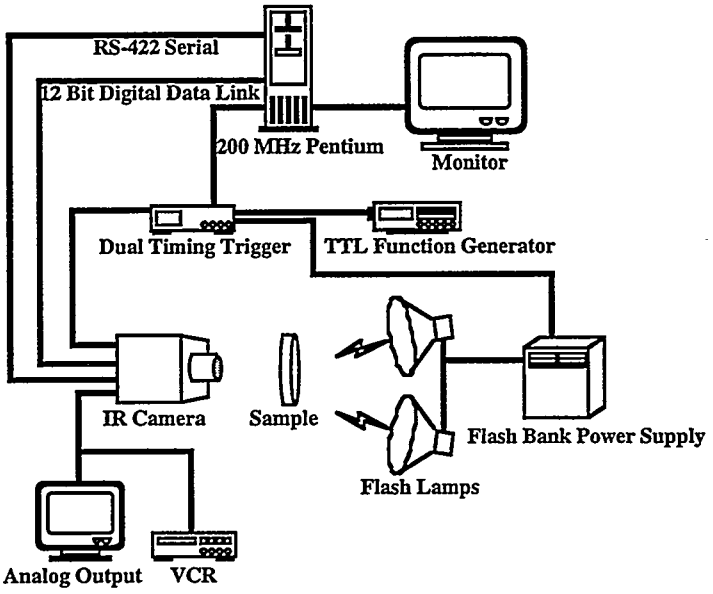

Fig. 1. Schematic diagram of experimental thermal imaging apparatus.

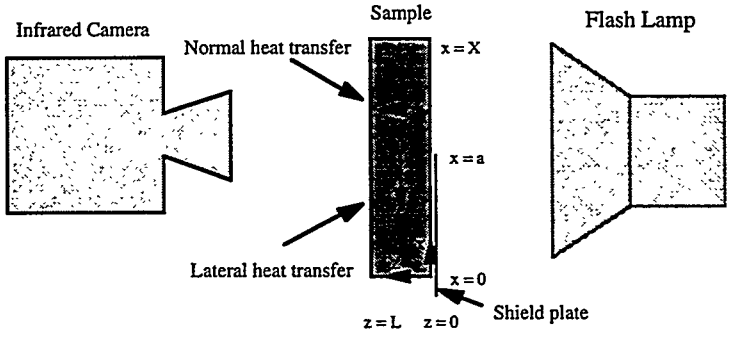

Fig. 2. Diagram of experimental setup for measuring lateral thermal diffusivity and notation for sample coordinates.

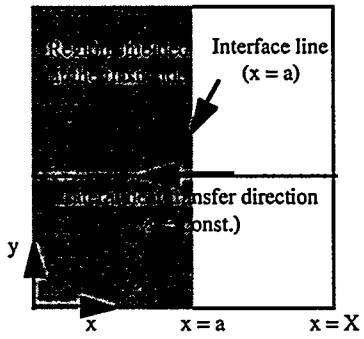

Fig. 3. Diagram of sample's front surface as viewed by the camera.

THEORY

For a semi-infinite ($0 < x < \infty$) sample of thickness L, Eq. 1 is the normalized analytical solution of the temperature distribution at the front surface ($z = L$) after an impulse heat source is applied on the back surface ($z = 0$), which is shielded in the region $0 < x < a$ (Ouyang et al., 1998). For a finite-width ($0 < x < X$) sample, we found the analytical solution of the temperature distribution as in Eq. 2. In Eqs. 1 and 2, α_x and α_z are the lateral and through-thickness thermal diffusivities, respectively. Figure 4 shows temperature distributions at an early time (t = 1 s) and a later time (t = 10 s) for a simulated sample calculated with Eqs. 1 and 2 and with the COMMIX numerical code (Domanus et al., 1990). It is seen that the finite-plate solution coincides with the numerical solution, while the semi-infinite solution deviates by 28.5% at t = 10 s.

$$T(x,L,t) = \frac{1}{2L}\left(\operatorname{erfc}\frac{a-x}{2\sqrt{\alpha_x t}} + \operatorname{erfc}\frac{a+x}{2\sqrt{\alpha_x t}}\right)\left[1 + 2\sum_{n=1}^{\infty}(-1)^n \exp\left(-\frac{n^2\pi^2}{L^2}\alpha_z t\right)\right] \tag{1}$$

$$T(x,L,t) = \frac{a}{XL}\left[1 + 2\sum_{m=1}^{\infty}\frac{X}{m\pi a}\sin\frac{m\pi a}{X}\cos\frac{m\pi x}{X}\exp\left(-\frac{m^2\pi^2}{X^2}\alpha_x t\right)\right]\left[1 + 2\sum_{n=1}^{\infty}(-1)^n \exp\left(-\frac{n^2\pi^2}{L^2}\alpha_z t\right)\right] \tag{2}$$

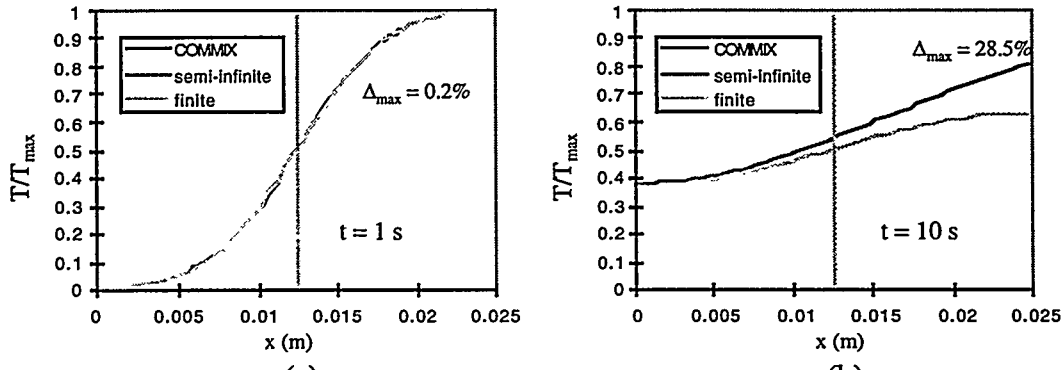

Fig. 4. Temperature distributions at (a) early time (t = 1 s) and (b) later time (t = 10 s) calculated from Eqs. 1 and 2 and from COMMIX numerical code.

The finite-width solution (Eq. 2) is then used to fit experimental data to determine the lateral thermal diffusivity. Transient data at each pixel are fitted first by the equation in the temporal domain to determine pixel amplitude, which may vary from pixel to pixel because of variations in sensor sensitivity and optical properties on the sample's surface. The temperature distributions at all time-steps are then fitted by the analytical solution to determine the two parameters: lateral thermal diffusivity α_x and interface location a, with least-squares fitting and Newton iteration scheme. The fitting function is defined as

$$F = \sum (T_{theo} - T_{exp})^2, \tag{3}$$

where T_{theo} and T_{exp} are the temperatures from the theoretical prediction and from experimental data, respectively. Figure 5 shows the variation of F with respect to α_x and a for an analytically generated data set. It is seen that a minimum (or best fit) exists at the theoretical values of $\alpha_x = 10$ mm^2/s and $a = 10$ mm.

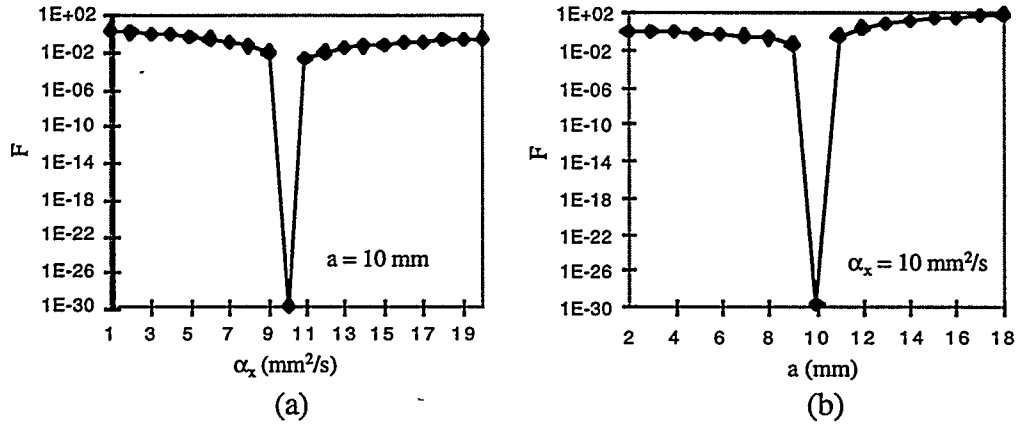

Fig. 5. Variation of fitting function $F = \sum (T_{theo} - T_{exp})^2$ with respect to (a) lateral thermal diffusivity α_x, and (b) interface location a as fitting parameters. With a perfect fit, F = 0.

RESULTS

Lateral thermal diffusivity was measured for two rectangular flat-plate samples, a steel plate, and an SiC/SiC CFCC plate. Average through-thickness thermal diffusivity for the steel plate was measured at 16.4 mm^2/s, and that for the SiC/SiC CFCC was 5.9 mm^2/s.

Figure 6 shows a time-series of infrared thermal images on the front surface of the steel plate after the thermal impulse has been applied at the back surface, which is shielded on the left side. The interface between the shielded and unshielded region is relatively sharp at the early time, but becomes blurred in the later times due to lateral heat transfer in the plate. The temperature distributions from this series of images are then fitted with the method described above for each horizontal line. Figure 7 shows typical results of the curve fitting between the experimental data and the analytical prediction based on Eq. 2. Average lateral thermal diffusivity is determined to be 16 mm^2/s.

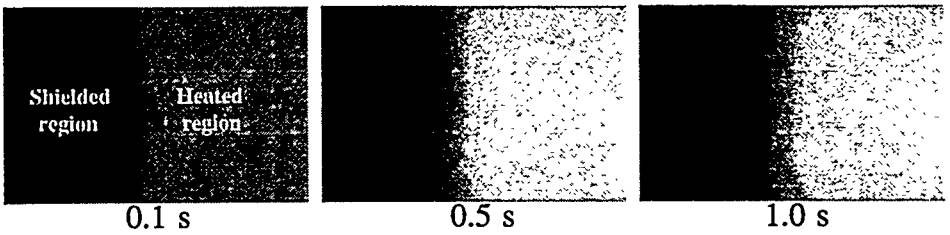

Fig. 6. Time-series of infrared thermal images on front surface of steel plate after application of thermal impulse at back surface.

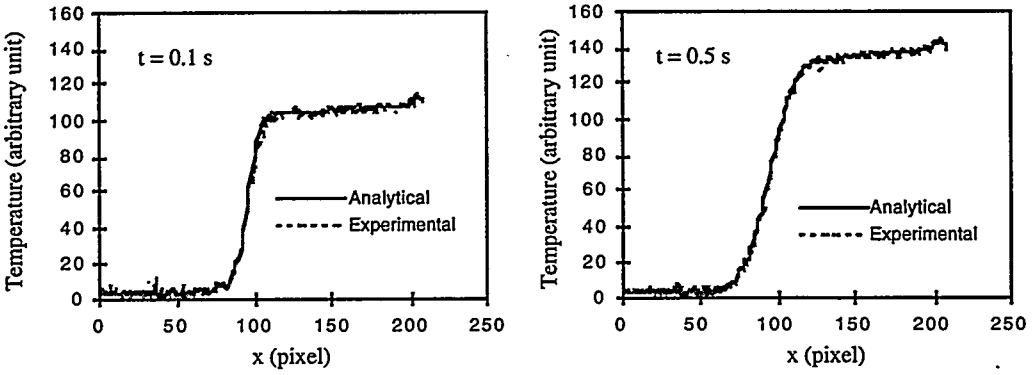

Fig. 7. Experimental data and analytical predictions from Eq. 2 for steel plate at (a) t = 0.1 s and (b) t = 0.5 s.

Figure 8 shows a time-series of infrared thermal images of the SiC/SiC CFCC plate, and Fig. 9 shows typical results of the curve fitting between the experimental data and the analytical prediction based on Eq. 2. It is seen that the experimental "temperature" distributions are not uniform. However, because the experimental data were obtained by an infrared camera, they represent the product of surface temperature and optical emissivity of the sample. The distribution pattern does not change with time, as seen in Fig. 9 for times of 0.25 and 0.95 s, so these nonuniform distributions should be attributed to optical emissivity variation on the sample surface. These apparent data variations are appropriately accounted for by the Argonne method. Average lateral thermal diffusivity is determined to be 7.5 mm^2/s, which is higher than the through-thickness thermal diffusivity of 5.9 mm^2/s because the fibers have higher thermal diffusivity and are aligned laterally.

Additional calibration and assessment of this technique is needed. The effects and sensitivities of convective cooling, noise intensity, and uneven heating, as well as determination of flash time, should be further evaluated.

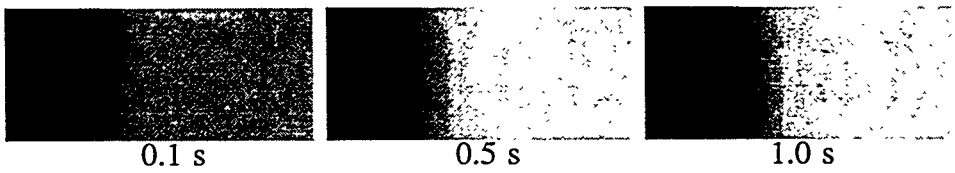

Fig. 8. Time-series of infrared thermal images on front surface of SiC/SiC CFCC after application of thermal impulse at back surface.

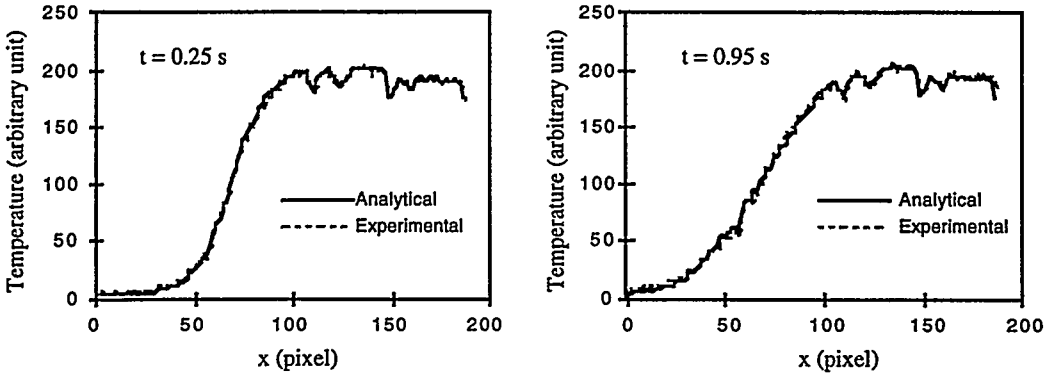

Fig. 9. Experimental data and analytical predictions from Eq. 2 for SiC/SiC CFCC plate at (a) t = 0.25 s and (b) t = 0.95 s.

CONCLUSIONS

A new technique has been developed at Argonne National Laboratory to measure lateral thermal diffusivity for planar samples of various sizes and materials. It is based on fitting of the experimental data with an analytical solution of the lateral heat transfer process. Initial measurements show good results for a steel plate and an SiC/SiC CFCC plate. This technique has been fully automated and can quickly determine the distributions of lateral thermal diffusivity. It may also be used as a nondestructive evaluation method to characterize subsurface defects.

ACKNOWLEDGMENTS

This work was funded by the U.S. Department of Energy, Energy Efficiency and Renewable Energy, Office of Industrial Technologies, under Contract W-31-109-ENG-38.

REFERENCES

Domanus, H. M., Cha, Y. S., Chien, T. H., Schmitt, R. C., and Shah, V. L., "COMMIX-1C: A Three-Dimensional Transient Single-Phase Computer Program for Thermal-Hydraulic Analysis of Single and Multicomponent Systems," NUREG/CR-5649, Argonne National Laboratory Report ANL-90-33, Sept. 1990.

Ouyang, Z., Zhang, F., Wang, L., Favro, L. D., and Thomas, R. L., "Novel Measurement of Anisotropic Thermal Diffusivity," in ***Review of Progress in QNDE, Vol 17***, eds. D. O. Thompson and D. E. Chimenti, pp. 453-456, 1998.

Parker, W. J., Jenkins, R. J., Butler, C. P., and Abbott, G. L., Flash method of determining thermal diffusivity, heat capacity, and thermal conductivity, ***J. Appl. Phys.***, 32:1679-1684, 1961.

Sun, J. G., Deemer, C., Ellingson, W. A., Easler, T. E., Szweda, A., and Craig, P. A., "Thermal Imaging Measurement and Correlation of Thermal Diffusivity in Continuous Fiber Ceramic Composites," in ***Thermal Conductivity 24***, eds. P. S. Gaal and D. E. Apostolescu, pp. 616-622, 1999.